Steel and Composite Structures, *Vol. 32, No. 4* (*2019*) *537-548*
DOI: https://doi.org/10.12989/scs.2019.32.4.537

Bond-slip effect in steel-concrete composite flexural members: Part 1 – Simplified numerical model

WonHo Lee [a], Hyo-Gyoung Kwak* and Ju-young Hwang [b]

Department of Civil and Environmental Engineering, Korea Advanced Institute of Science and Technology, 291 Daehak-ro, Yuseong-gu, Daejeon 34141, Republic of Korea

(*Received March 7, 2019, Revised July 13, 2019, Accepted August 22, 2019*)

Abstract. This paper introduces an improved numerical model which can consider the bond-slip effect in steel-concrete composite structures without taking double nodes to minimize the complexity in constructing a finite element model. On the basis of a linear partial interaction theory and the use of the bond link element, the slip behavior is defined and the equivalent modulus of elasticity and yield strength for steel is derived. A solution procedure to evaluate the slip behavior along the interface of the composite flexural members is also proposed. After constructing the transfer matrix relation at an element level, successive application of the constructed relation is conducted from the first element to the last element with the compatibility condition and equilibrium equations at each node. Finally, correlation studies between numerical results and experimental data are conducted with the objective of establishing the validity of the proposed numerical model.

Keywords: composite structure; bond-slip; slip analysis; flexural member; FEM

1. Introduction

Steel-concrete composite structures have been widely used in various structures such as bridges and buildings, owing to the fact that each material of steel or concrete is used to take advantage of its best attributes to make composite structures very efficient and economical. However, these benefits of composite structures are based on having an efficient connection between the steel and concrete components, introduced in the form of mechanical shear connectors (Oehlers and Bradford 1999), because the shear connectors allow the shear transfer of the forces in concrete to steel and vice versa, and also prevent vertical separation of the steel and concrete components.

Since the deformations, stress distributions, and failure modes of composite structures deeply depend on the behavior of the shear connection, various experimental and numerical studies of the slip behavior along the shear connectors have been extensively performed (Bärtschi and Fontana 2006, Bonilla *et al*. 2018, El-lobody and Lam 2002, Lin *et al*. 2017, Winkler *et al*. 2006), and the obtained results have been implemented in the design codes such as AISC (2010) and Eurocode (2004). In particular, differently from civil structures usually designed with complete shear connection, building structures frequently adopt a partial shear connection, which causes a significant redistribution of stresses along the interface between the steel and concrete components and affects the ultimate resisting capacity as well as the serviceability. This means that the slip behavior along the interface between the steel and concrete components cannot be ignored in the analysis and design of steel-concrete composite structures.

To verify the slip behavior in the composite structures, many experimental studies have been performed (Bärtschi and Fontana 2006, Ding *et al*. 2017, Lam and El-Lobody 2005, Loh *et al*. 2004), and Oehlers and Coughlan (1986) introduced a criterion to determine the strength of a shear stud at a partial composite state, and suggested the empirical load-slip relation of the shear stud on the basis of 116 push-out tests. In addition, many analytical approaches to address a decrease in the resisting capacity and an increase in the deflection in the composite structures with a partial shear connection have been explored. Dezi *et al*. (1993) directly solved the governing differential equations by using the finite differential method to calculate the deflection change caused by the slip between the steel beam and concrete slab, and Roberts (1985) obtained slip and nodal displacements for typical composite beams with use of the finite differential method (FDM) constructed on the basis of the force equilibrium and compatibility condition. These numerical approaches generally yield very accurate results and are very useful in the analysis of partially composite structures, but also have numerous restrictions in application since the solution procedure is strongly dependent on the governing equation and boundary conditions.

To overcome those limitations in considering the slip behavior in the partially composite structures, a few numerical models have been proposed on the basis of the finite element method (FEM) (Dias *et al*. 2015, Gara *et al*. 2006, Ranzi and Zona 2007, Sousa and da Silva 2007,

*Corresponding author, Professor,
E-mail: khg@kaist.ac.kr
[a] Ph.D. Student
[b] Ph.D.

ISSN: 1229-9367 (Print), 1598-6233 (Online)

Wang and Chung 2008), and the slip behavior has been simulated through the springs connected at the interface between the steel and concrete components. The direct adoption of the spring elements (Gattesco 1999, Queiroz *et al*. 2007), however, requires the use of a double node to represent the relative slip between both components. In spite of easy application into the finite element formulation, this method leads not only to an increase in the number of degrees of freedom but also to greater complexity in the mesh definition, especially in the case of a structure with numerous nodes and elements (Hwang and Kwak 2013). These restrictions in numerical modeling of the composite structures have discouraged researchers from including the slip effect in many previous numerical studies.

To address this issue, this paper introduces an improved numerical approach that can consider the bond-slip effect without taking the double nodes along the interface between the steel and concrete components by incorporating the equivalent stiffness E_s^{EQ} and yield strength f_y^{EQ} of steel. In advance, the slip behavior is analyzed on the basis of a linear partial interaction theory (Oehlers and Bradford 1999). Upon deriving the governing equation for the slip behavior, the transfer matrix relation is constructed at an element level, and the successive application of the compatibility condition and equilibrium equations at each node makes it possible to determine the nodal forces and displacements related to the slip behavior. The reliability of the proposed approach is verified by comparing the analytical predictions with results from experiments, and this approach can also be implemented into commercialized programs including ABAQUS (Simulia 2017) and ADINA (2015) as a user defined material model.

2. Material properties

Since the bending response of steel-concrete composite beams and/or slabs subjected to monotonic loadings is much more affected by the tensile behavior than by the compressive behavior of concrete, the stress-strain relation of concrete in compression is not of primary interest and can be defined with the use of a simplified relation. Among the numerous mathematical models used in the numerical analysis of concrete structures, accordingly, the monotonic envelope curve of stress-stain for concrete introduced by Kent and Park and later modified by Scott *et al*. (1982) is adopted in this paper, because of its simplicity and computational efficiency. This model describes the monotonic concrete stress-strain relation in compression as a second-degree parabola accompanying the linear descending branch after reaching the compressive strength, as shown in Fig. 1.

On the other hand, the tensile behavior of concrete is assumed to be linear elastic until reaching the tensile strength. After the tensile strength, the tensile stress decreases linearly with increasing principal tensile strain to ε_0 in Fig. 1, which is expected as the ultimate failure strain by cracking (Kwak and Kim 2010). To describe the cracking behavior, the damaged plasticity model (Lubliner *et al*. 1989) among the cracking models defined in

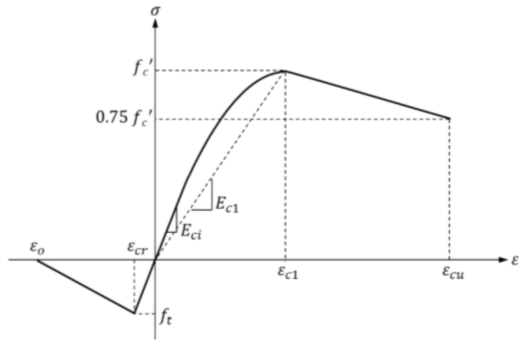

Fig. 1 Stress-strain relation of concrete

ABAQUS is adopted because this model shows not only less sensitivity to the mesh topology but also stable convergence to the solution even in the local failure zone where a stress concentration is expected.

Steel is modeled as a linear elastic, linear strain hardening material with yield stress f_y. The reasons for this approximation are: (1) computational convenience of the model; and (2) the behavior of composite structures is greatly affected by yielding of the steel component. It is, therefore, advisable to take advantage of the strain hardening behavior of steel in improving the numerical stability of the solution. More details of the material models for concrete and steel can be found elsewhere (Kent and Park 1971, Kwak and Hwang 2010).

3. Implementation of slip behavior

3.1 Load-slip relation of stud connection

The entire structural responses from the flexural deformation to the slip behavior in steel-concrete composite flexural members are greatly influenced by the shear connectors because composite flexural members are equipped with shear connectors along the interface between a steel component and a concrete component to unify the behavior of the total structure. A dense arrangement of the shear connectors leads to a perfect bond condition but a loose arrangement allows the occurrence of slip along the interface.

Since the behavior of slip is usually represented by the relation between the longitudinal shear load at the interface and the corresponding slip, many push-out tests for shear connectors especially for the stud connector, one of the most commonly used types of mechanical shear connector, have been performed to obtain the load-slip relations (Menzies 1971, Oehlers and Coughlan 1986, Shim *et al*. 2004). As well documented in many experimental studies, a typical load-slip relation represents the linear variation nearly up to half of the ultimate strength. When slip increases further, the stiffness is reduced gradually and eventually reaches the ultimate shear strength (see dashed line in Fig. 2). Among a number of proposed empirical relations, a simple bilinear load-slip relation of the stud connector (see the continuous line in Fig. 2) is adopted in this paper for computational convenience. The maximum

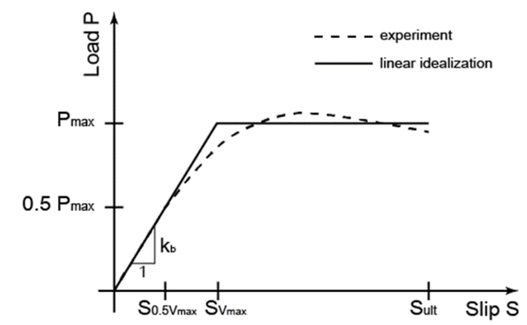

Fig. 2 Idealized load-slip relation of a shear stud

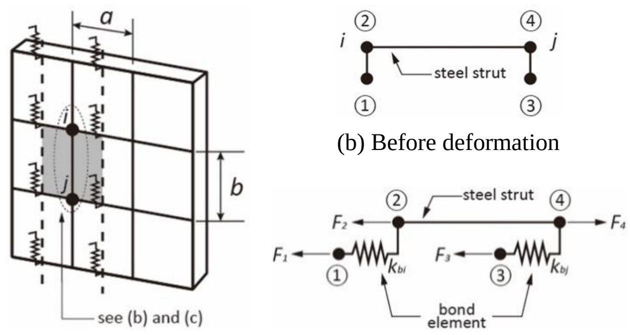

(a) A part of steel component (b) Before deformation (c) After deformation

Fig. 3 An idealized steel strut with bond-slip

shear force P_{max} is determined by $P_{max} = 0.8 f_u (\pi d_{sh}{}^2 4)/1.25$ mentioned in Eurocode 4 (2004), where d_{sh} is the diameter of the shear connector and f_u is the ultimate tensile strength of studs.

Concerning the linear behavior of the stud connector, the slip S corresponding to the applied horizontal shear force P(x) can be represented by Eq. (1) if the shear studs are assumed to be installed with uniform spacing L_S in the longitudinal direction.

$$\mathrm{S} = \frac{P(x)}{k_b} = \frac{q(x) \cdot L_s}{k_b} \tag{1}$$

where k_b is the stiffness of the shear stud (see Fig. 2) and q(x) is the shear force transmitted per unit length of the structural member. This is known as the shear flow (q(x) = dP(x)/dx).

3.2 Evaluation of equivalent stiffness and yield strength of steel

To take into account the bond-slip behavior, defined by the displacement difference between a steel component and a concrete component in a composite structure, two basically different elements, the bond link element (Keuser and Mehlhorn 1988) and the bond zone element (de Groot *et al*. 1981) have been used in the finite element analyses (Dehestani and Mousavi 2015, Kwak and Kim 2001, Lowes *et al*. 2004). In spite of their ease of use, however, these elements necessitate the usse of a double node to represent the relative slip between the two components. In a complex structure, this requirement leads to not only a considerable increase in the number of degrees of freedom but also greater complicatedness of the mesh definition and has discouraged researchers from including the bond-slip effect in many studies to date.

To address these limitations in using the classical bond-slip elements, an equivalent steel stiffness that includes the bond-slip deformation is proposed in this paper. After separating a composite structure into two parts of the steel and concrete components, bond slip effect is taken into consideration by modifying the material properties of the steel component. As shown in Fig. 3(a), which represents a part of the steel component discretized with the finite element mesh size of *ab*, the steel area covered by the adjacent two nodes of node *i* and node *j* can be considered as an equivalent strut or tie. A convenient free body diagram that isolates the steel strut with the bond-link elements attached at its end points is then selected. Figs. 3(b) and 3(c) show this element before and after deformation, where points ① and ③ are associated with the concrete component and points ② and ④ are associated with the steel component at nodes *i* and *j*, respectively. The corresponding degrees of freedom of the steel strut and concrete at each end are connected by the bond-link element, whose stiffness depends on the relative displacement between the steel component and the concrete component. With this assumption, the stiffness matrix that relates the end displacements along the axis of the steel component with the corresponding forces can be expressed as follows

$$\begin{Bmatrix} F_c \\ F_s \end{Bmatrix} = \begin{Bmatrix} F_{①} \\ F_{③} \\ F_{②} \\ F_{④} \end{Bmatrix} = \begin{bmatrix} k_{bi} & 0 & -k_{bi} & 0 \\ 0 & k_{bj} & 0 & -k_{bj} \\ -k_{bi} & 0 & k_s + k_{bi} & -k_s \\ 0 & -k_{bj} & -k_s & k_s + k_{bj} \end{bmatrix} \cdot \begin{Bmatrix} u_{①} \\ u_{③} \\ u_{②} \\ u_{④} \end{Bmatrix} = \begin{bmatrix} K_{CC} & K_{CS} \\ K_{CS} & K_{SS} \end{bmatrix} \begin{Bmatrix} u_c \\ u_s \end{Bmatrix} \tag{2}$$

where, $k_s = at/b \cdot E_S$ is the strut stiffness, k_{bi} and k_{bj} are the stiffness of the bond-link element determined in Eq. (1), and *t* is the thickness of the steel component.

By considering the steel degrees of freedom in Eq. (2), the following relation between concrete displacements and corresponding forces results in $\{F_c^*\} = [K_{CC}{}^*]\{u_c\}$, where $\{F_c^*\} = \{F_c\} - [K_{CS}] \cdot [K_{SS}]^{-1} \cdot \{\mathrm{F_s}\}$, $[K_{CC}{}^*] = [K_{CC}] - [K_{CS}] \cdot [K_{SS}]^{-1} \cdot [K_{CS}]$. After evaluating the inverse of $[K_{SS}]$ and carrying out multiplications, the equivalent stiffness $[K_{CC}{}^*]$ is reduced to the following

$$\left[K_S{}^{EQ}\right] = [K_{CC}{}^*] = \frac{k_s k_{bi} k_{bj}}{k_s(k_{bi} + k_{bj}) + k_{bi} \cdot k_{bj}} \begin{bmatrix} 1 & -1 \\ -1 & 1 \end{bmatrix} \tag{3}$$

which is the local stiffness matrix of the steel strut element including the effect of bond-slip, and it is now apparent that bond-slip reduces the stiffness of the steel strut element. Even when the steel component is modeled with plate or shell elements, its stiffness is directly proportional to the modulus of elasticity. Therefore, the equivalent modulus of elasticity for the steel component can be inferred from Eq. (3) as

$$E_s^{EQ} = \frac{E_s k_{bi} k_{bj}}{at/b \cdot E_s\left(k_{bi} + k_{bj}\right) + k_{bi} \cdot k_{bj}} \tag{4}$$

In the case of a perfect bond, the bond stiffness terms k_{bi} and k_{bj} become infinitely large and the equivalent modulus of elasticity E_S^{EQ} is increased to the elastic modulus of elasticity E_S. The use of E_S^{EQ} instead of E_S makes it possible to consider the bond-slip effect without taking double nodes along the interface between the steel component and the concrete component. The substitution of the new material properties of steel and bond into Eq. (4) yields the equivalent elastic modulus of the steel component. In particular, differently from the linear load-slip assumption considered in this paper, the use of any nonlinear load-slip relation makes it possible to take into account the change in the slip modulus after exceeding the elastic limit.

Even though the equivalent steel stiffness E_S^{EQ} introduced in this paper can effectively describe the stiffness of the composite structure when the bond-slip effect is considered, there is a limitation in describing a decrease of the resisting capacity due to the partial shear connection. The proposed model cannot directly simulate the strength degradation caused by longitudinal slip or vertical separation because the model assumes a perfect bond at the interface. Nevertheless, upon adopting the equivalent yield strength of steel $\left(E_S^{EQ}\right)$, it is possible to consider a decrease of the resisting capacity due to shear stud failure or buckling of the steel plate.

When the strength of shear stud is weaker than the yield strength of the steel plate, shear failure occurs prior to yielding of the steel plate and the shear force can no longer be transferred between the steel plate and the interior concrete matrix. Therefore, the maximum axial force that can act on a steel-concrete composite structure is determined based on the minimum of the strength of exterior steel plate and the strength of shear connection (Roberts *et al*. 1995). Accordingly, if the shear connection is sufficient, the yield strength of the exterior steel plate will directly be used as the equivalent yield strength. Otherwise the yield strength of the steel in the proposed model will be modified as shown in Eq. (5) such that the yield strength of steel plate is limited to the strength of shear connection, where n is the number of studs in the effective length, P_{max} is the maximum strength of a single stud determined from experiments or design codes (Eurocode 2004) and A_s is the cross-section area of exterior steel plate.

$$\left(f_y^{EQ}\right)_{stud} = min\left(f_y\, , nP_{max}/A_s\right) \tag{5}$$

Different from a usual steel-concrete composite beam in which the concrete slab and the steel beam are designed to resist the compressive force and tensile force respectively, the resisting capacity of a steel-concrete sandwich panel in which both steel plates are attached to both sides of the concrete matrix will be dominantly affected by the buckling of steel plate on the compression side. Since the steel plate cannot resist additional stress after buckling has occurred, additional modification for the yield strength of steel must be considered if the critical stress is smaller than the yield strength of the steel plate. Zhang (2014) suggested using Euler's column buckling equation with an effective length coefficient k equal to 0.7 to represent the critical stress $\sigma_{cr} = \pi^2 E_s/(12k^2(s/t)^2)$ for the steel-concrete sandwich panel, where E_s is the elastic modulus of the steel plate, s is the stud spacing, and t is the thickness of the steel plate. Therefore, the equivalent yield strength of steel plate under compression is evaluated as Eq. (6). From Eqs. (5) and (6), the equivalent yield strength of the steel plate can finally be determined as $f_y^{EQ} = min\left(\left(f_y^{EQ}\right)_{stud},\ \left(f_y^{EQ}\right)_{buckling}\right)$

$$\left(f_y^{EQ}\right)_{buckling} = min\left(f_y\, , \pi^2 E/(12k^2(s/t)^2)\right) \tag{6}$$

In the proposed model, the stiffness and strength of the composite flexural members are predicted by adopting the equivalent stiffness and yield strength of steel. Nevertheless, the slip distribution along the span is still not determined. To supplement this limitation and to make evaluation of the slip behavior possible, a solution algorithm for the bond slip analysis is designed and accompanied in this paper.

3.3 Solution algorithm for the analysis of slip behavior

Once the displacement and internal force increments at each node are determined for the current load increment, evaluation of the slip behavior along the interface between the steel component and the concrete component is followed. When a composite flexural member is subjected to lateral loads, the bending moment M(x) and shear force V(x) can be calculated at any section located at distance x from the support (see Fig. 4(a)), and the internal moment M(x) will develop the curvature κ in the corresponding section (see Fig. 4(b)). If the interface slip between the steel component and the concrete component is not totally prevented, the longitudinal strains of both components at the interface have different values from each other. Figs. 4(b) and (c) show the strain and corresponding stress distribution across the section of a composite flexural member with partial bond. However, it will still be assumed that there is no separation between the two components, which means the curvatures of two components are identical.

As shown in Fig. 4(c), when any section of a composite flexural member is subjected to axial force F and moment M, which act through the centroids of the concrete and steel components at distances h_c and h_s from the steel-concrete interface, respectively, the elastic strains ε_{cb} at the bottom face of the concrete component and ε_{st} at the top face of the steel component can be obtained from the elastic beam theory by

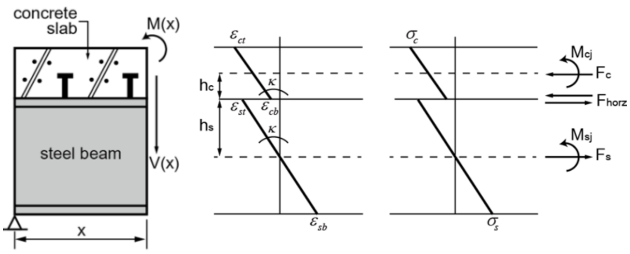

(a) A typical section (b) Strain distribution (c) Stress distribution

Fig. 4 Slip behavior in partially composite beam

$$\varepsilon_{cb} = -\frac{F_c}{E_c A_c} + \frac{M_c h_c}{E_c I_c}, \quad \varepsilon_{st} = \frac{F_s}{E_s A_s} - \frac{M_s h_s}{E_s I_s} \tag{7}$$

where A_s and A_c represent the areas of the steel and concrete components, respectively, while I_s and I_c are the moments of inertia of the cross-sectional area of each component with respect to their centroidal axes.

From the horizontal force equilibrium which requires that $\sum F = 0$, F_s must be the same as F_c (see Fig. 4(c)). In addition, the distribution of forces in the shear connectors can be determined by detaching the concrete component from the steel component. If a reference section of zero moment is chosen, namely the section at the external supports or at the contra-flexural points in a continuous flexural member, the total horizontal force on the shear connectors F_{horz} must equal the normal force at each component. That is, the relation of $F_s = F_c = F_{horz}$ can be obtained from simple horizontal force equilibrium.

As mentioned above, when the composite section is subjected to the bending moment, the relative movement across the interface that is induced by the sliding action is referred to as the slip of $\mathrm{S} = u_s - u_c$, and the derivative of this relation with respect to the longitudinal distance *x* yield a slip strain of $\varepsilon_{slip} = dS/dx = \varepsilon_{st} - \varepsilon_{cb}$. Hence, from Eqs. (1) to (4) and (7), the following differential equation represented by the material constants and section dimensions can be obtained.

$$\frac{L_s}{k_b}\frac{d^2 F_{horz}}{dx^2} = F_{horz}\left(\frac{1}{E_c A_c} + \frac{1}{E_s A_s}\right) - \left(\frac{M_c h_c}{E_c I_c} + \frac{M_s h_s}{E_s I_s}\right) \tag{8}$$

From the rotational equilibrium of the internal moment, the total moment $\mathrm{M(x)}$ at the section being considered in Fig. 4 can be expressed by $\mathrm{M(x)} = M_c(x) + M_s(x) + F(x)_{horz}(h_c + h_s)$. Moreover, the introduced assumption for the identical curvatures of two components leads to $\kappa = \frac{M_c}{E_c I_c} = -\frac{1}{d_c}(\varepsilon_{ct} - \varepsilon_{cb})$ where d_c means the thickness of the concrete component. These two relations for $\mathrm{M(x)}$ and κ make it possible to express the curvature κ at a section located at distance xfrom the far end support in terms of internal force components as $\kappa = \{M(x) - F(x)_{horz}(h_c + h_s)\}/\sum EI$, where $\sum EI = E_c I_c + E_s I_s$. Eq. (8) yields the following ordinary linear differential equation for $F(x)_{horz}$ in advance.

$$\frac{d^2 F(x)_{horz}}{dx^2} - \frac{k_b}{L_s}\frac{EI^*}{EA^* \sum EI} F(x)_{horz} = -\frac{k_b}{L_s}\frac{(h_c + h_s)}{(E_c I_c + E_s I_s)} M(x)$$

where

$$\frac{1}{EA^*} = \frac{1}{E_c A_c} + \frac{1}{E_s A_s} \tag{9}$$

and

$$EI^* = \sum EI + EA^*(h_c + h_s)^2$$

This constructed governing equation can also be rewritten as

$$\mathrm{F}''(\mathrm{x}) + \mathrm{K} \cdot \mathrm{F}(\mathrm{x}) = \mathrm{p}(\mathrm{x})$$

where

$$\mathrm{K} = -\frac{k_b}{L_s}\frac{EI^*}{EA^* \sum EI}$$

and

$$\mathrm{p}(\mathrm{x}) = -\frac{k_b}{L_s}\frac{(h_c + h_s)}{(E_c I_c + E_s I_s)}\mathrm{M}(\mathrm{x}) = -\frac{k_b}{L_s} \cdot Q \cdot M(x) \tag{10}$$

However, this approach is limited to the composite flexural members without axial deformations due to the pre-stressing force or time-dependent deformations such as the creep and shrinkage of concrete. In the case of considering the axial deformations, all the derivation procedures from the numerical formulation to the force equilibrium mentioned in this paper should be modified to take into account the axial load effect.

3.4 Solution procedure for bond-slip analysis

After determination of internal forces at each loading step through the same solution procedures with those used in a typical non-linear finite element analysis (Gattesco 1999), the bond-slip behavior in a composite structure is evaluated according to the analysis flow described in Fig. 5. As a result of the bond-slip analysis, the horizontal shear force developed along the interface of composite flexural members and the bond-slip distribution are determined and, in advance, the discontinuous strain distribution in the section can also be computed.

Since the constructed governing equation of Eq. (10) is equivalent to the dynamic equation of motion $\mathrm{M} \cdot \mathrm{U}''(\mathrm{t}) + \mathrm{C} \cdot \mathrm{U}'(\mathrm{t}) + \mathrm{K} \cdot \mathrm{U}(\mathrm{t}) = \mathrm{p}(\mathrm{t})$ with $\mathrm{M} = 1.0$ and $\mathrm{C} = 0.0$, it is possible to use one of the direct numerical integration methods that are popularly used in structural dynamic analysis (Chopra 2007). The average acceleration method of Newmark's method on the basis of the non-iterative formulation is adopted in this paper, and more details of the solution procedure can be found elsewhere (Bathe 2007).

Upon the assumptions that the horizontal force and corresponding relative slip are continuous along the span length and the structure is subdivided into *n* elements, the continuous distribution of moment determined through a numerical analysis such as a beam analysis can be assumed

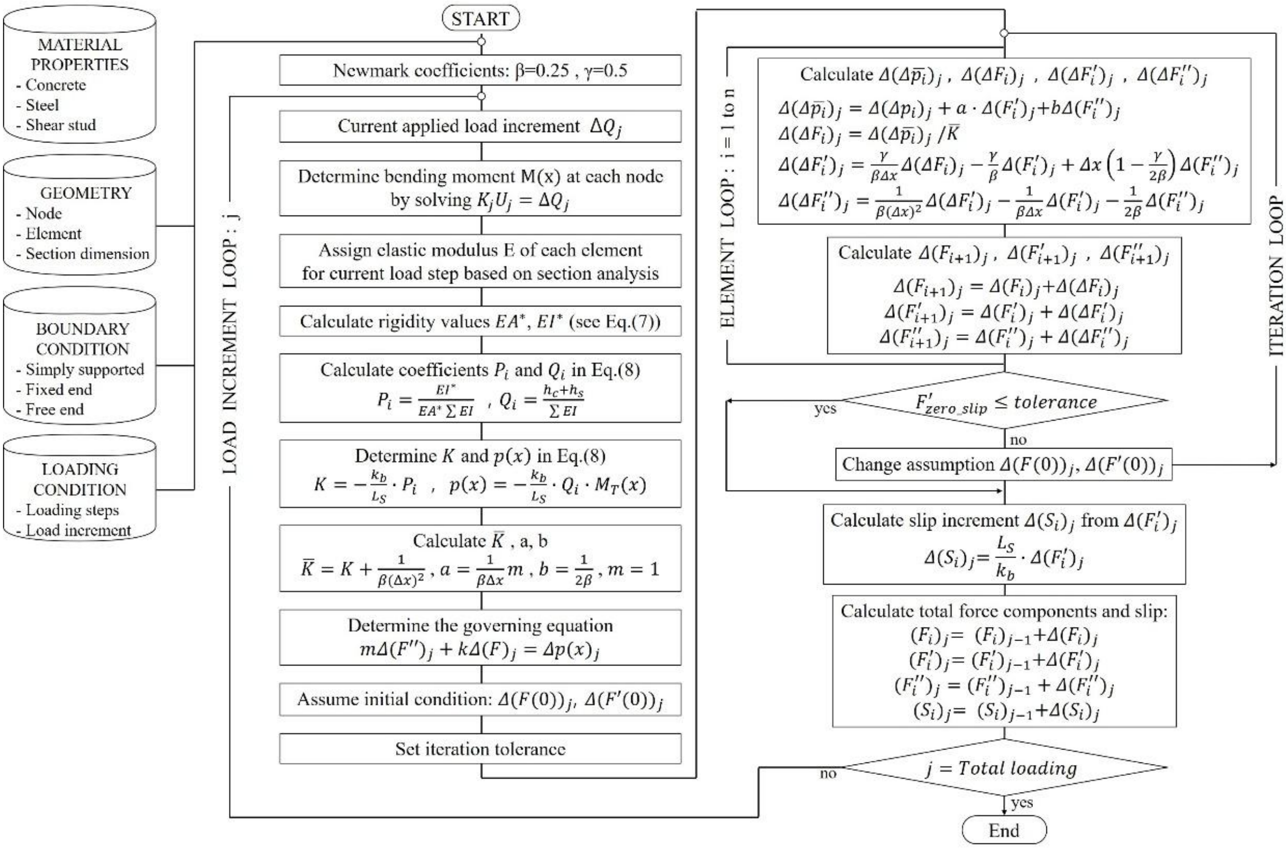

Fig. 5 Flow chart for bond-slip analysis

to be linear at each element. Once the moment value required to evaluate the component of $p(x)$ in Eq. (10) is determined, the transfer solution procedure is followed.

Considering that the first step of the solution procedure for the dynamic equation is started from the evaluation of the initial acceleration $U''(0)$ on the basis of the initial conditions of $U'(0)$ and $U(0)$, the solution procedure for Eq. (10) is initiated with the assumption for $F'(0)$ and $F(0)$ at one end of the first element in a structure, and gives increments for ΔF, $\Delta F'$ and $\Delta F''$ at the first element. The superposition of these increments into the assumed initial conditions will serve as the boundary conditions for the second element, and this sequential solution procedure can advance until reaching the far end of the structure. If the obtained value at the other end point does not satisfy the given boundary condition, then the same solution procedure is restarted with the change in the assumption for $F'(0)$ and $F(0)$. This iteration is repeated until reaching the converged result, and the flow diagram of Fig. 5 shows some details related to the analysis of slip behavior.

4. Verification of proposed bond-slip model

The verification of the proposed bond-slip model has been performed through comparison of the numerical results with experimental data for shear connectors and analytical solution for a composite beam.

ABAQUS 6.17 (Simulia 2017) is used in the numerical analyses, and 8-node 3D solid elements (named C3D8R element in ABAQUS) are adopted in the numerical modeling of both steel and concrete components. Moreover, to ensure consistency in the numerical modeling of all of the specimens considered in this paper, the mesh size of each finite element is based on an equal length of 20 mm regardless of the difference in the specimen size. The dimensions of 20 mm × 20 mm × 20 mm are chosen for the modeling of the concrete matrix, and this size is determined through a convergence test for the FE mesh size. The same principle underlying numerical modeling is also applied to the steel plate.

4.1 Slip behavior of stud shear connectors

First, in order to investigate the validity of the proposed slip model, the experimental results of stud shear connectors tested by Shim *et al*. (2004) have been compared. This test specimen was designed according to the description for the standard push-out test specimen defined in Eurocode 4 (2004), and Figs. 6 and 7 show details of the configuration and corresponding finite element idealization of the test specimen. In particular, since bonding at the interface between the concrete slab and the steel beam was prevented by greasing the flange of the steel beam because the object of this experiment was to derive the load-slip relation of a stud shear connector, no bond between the steel plate and concrete matrix was assumed in numerical modeling of the specimen. The compressive strength of concrete is 49.3 MPa, and the shear stud with a diameter of 25 mm has a yield strength of 328

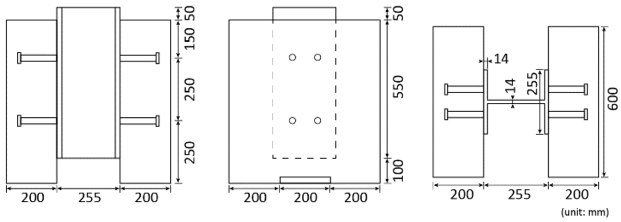

Fig. 6 Configuration of test specimen

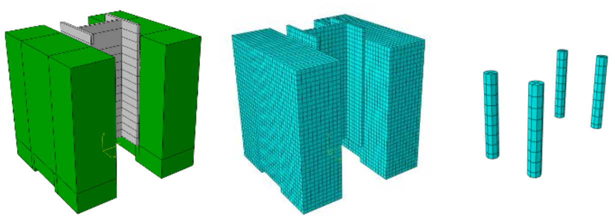

(a) FE model (b) Mesh of FE model (c) Mesh of studs

Fig. 7 Finite element idealization

MPa and a tensile strength of 426 MPa. In advance, $E_c = 40$ GPa and $E_s = 213$ GPa are used for concrete and steel components upon the experiment. More details related to the experiment can be found elsewhere (Shim *et al*. 2004).

Fig. 8 shows the numerical prediction of the developed slip (Curve B in Fig. 8) compared with the experimental data (Curve A in Fig. 8) and it indicates that the application of the finite element idealization adopted in this paper is sufficient to exactly simulate the slip behavior by the shear studs along the interface between the steel and concrete components. In advance, to simplify the numerical formulation for the slip behavior, the linearized load-slip relation of Curve C in Fig. 8 is introduced and Curve D shows the corresponding numerical results obtained by assuming a perfect bond between the steel and concrete components upon the use of the equivalent steel stiffness at the flange area of the steel beam. For reference, moreover, the numerical prediction obtained by assuming a perfect bond along the interface without considering the equivalent steel stiffness is added as Curve E.

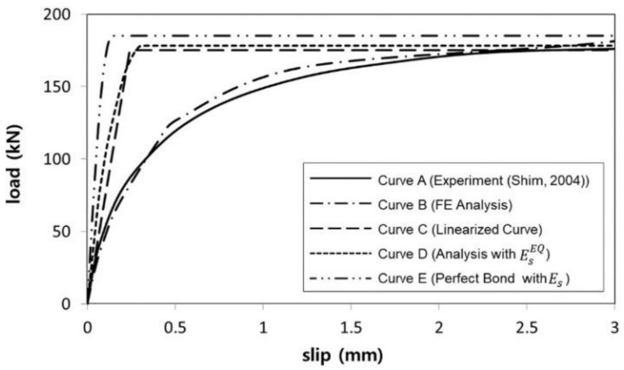

Fig. 8 Load-slip relation of shear stud

This figure not only gives very satisfactory agreement between the results of the analyses and experimental data but also demonstrates the applicability of the introduced model of the equivalent steel stiffness. In particular, the introduced model, which does not use double nodes, can yield significant savings in the number of degrees of freedom required to account for the bond-slip effect and will remove the difficulty arising in constructing a FE mesh in three dimensional FE modeling. On the other hand, this figure also shows that the numerical results determined on the basis of the perfect bond assumption present remarkable differences from the experimental data, and this indicates that the perfect bond assumption has a limitation in predicting the structural behavior of composite structures. Accordingly, the bond-slip effect must be considered to exactly evaluate the composite action of structures. In advance, the equivalent steel stiffness can effectively be used to simulate the bond-slip behavior without taking the double nodes.

4.2 Slip behavior of composite flexural beam

Because there is little experimental data for the slip behavior along the interface of composite flexural members, comparisons of the partial slip behavior for the verification of the numerical model mentioned in Eq. (10) were conducted with the analytical results introduced by Oehlers and Bradford (2013), Kwak and Hwang (2010). The first example structure is a simply supported one span beam with a span length of 12 m that is subjected to a concentrated load of 9.8 kN at the mid-span. The geometry and sectional dimensions are shown in Fig. 9, and the material properties used are $K_s/L_s = 150$ MPa, $E_c = 33.3$ GPa and $E_s = 200$ GPa. The concrete slab and steel beam are assumed to behave linearly up to its compressive strength and yield strength, respectively, as was assumed in a previous study (Kwak and Hwang 2010).

As shown in Fig. 10, the numerical results obtained in this paper show good agreement with the analytical solutions by Oehlers and Bradford (2013), and the difference in the maximum structural response between the numerical results and those of previous researchers (Roberts 1985) is hardly noticeable. This means that the introduced numerical model can effectively simulate the slip behavior along the interface of composite flexural members. Moreover, differently from the analytical approach which requires the predetermined known boundary conditions to obtain a closed form solution, the introduced numerical model has no restriction in application to various structures subjected to arbitrary lateral loadings due to the use of the iterative solution scheme.

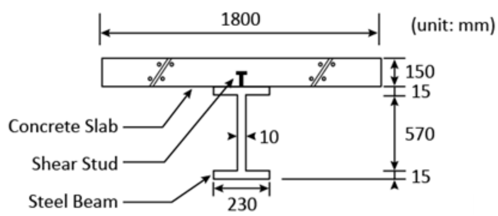

Fig. 9 Cross section of the example structure

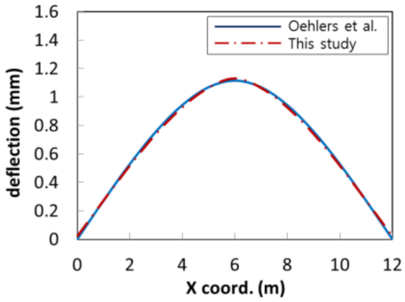

(a) Deflection

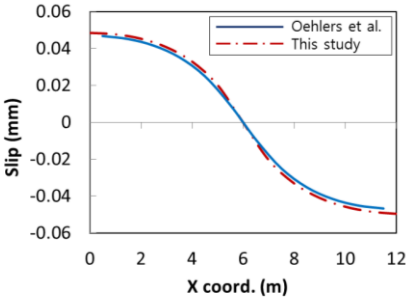

(b) Slip

Fig. 10 Structural response of the example structure

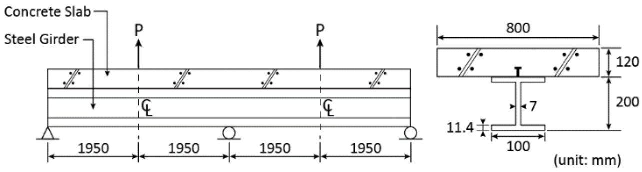

Fig. 11 Two-span continuous composite beam CCB4

In the case of this example structure, the boundary conditions for the horizontal shear force are already known at both end points ($F(0) = 0$ and $F(L) = 0$), and the iteration starts with the initial assumption for the slip at $x = 0$ ($F'(0) = 0$). The sequential application of Eq. (10) from the first element to the last element then yields the horizontal force and slip at the other end point at $x = L$. As one boundary condition at that end is already known ($F(0) = 0$), the initial assumption of $F'(0)$ needs to be corrected until $F(L/2) = 0$ is satisfied based on the boundary condition and symmetry. More details related to the iteration procedure can be found in Fig. 5.

In addition, a comparison of the two-span continuous beam CCB4 in Fig. 11, which was tested by Lizhong *et al.* (2008) and numerically analyzed by Hwang and Kwak (2013), is conducted. Two concentrated loads of P = 20 kN are applied at the middle of each span, and the values of the modulus of elasticity for concrete and steel are assumed to be the same as those used in the previous example structure. However, studs in beam CCB4 are equipped at different distances for three areas: $L_s = 90$ mm from the end support to the position where a load is applied; $L_s = 70$ mm from the load-position to the position where the

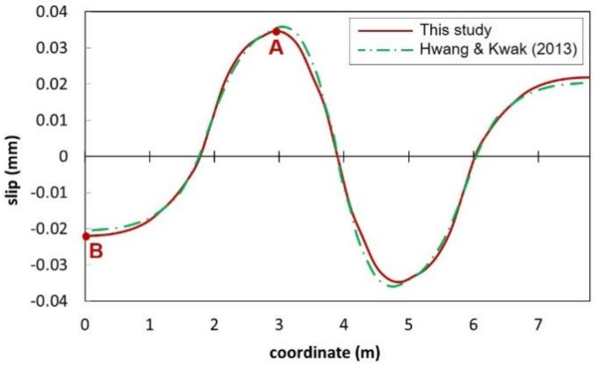

(a) Slip distribution

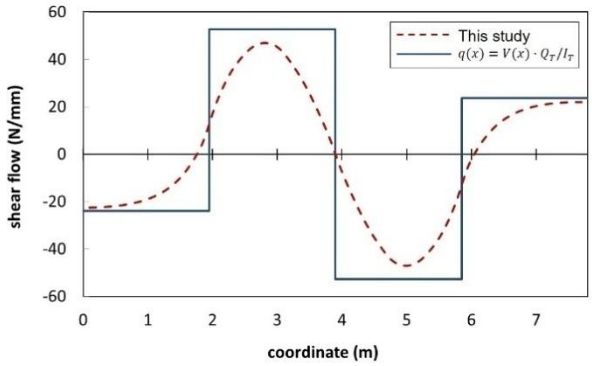

(b) Horizontal shear flow distribution

Fig. 12 Slip and shear flow distribution of beam CCB4

bending moment is zero; and $L_s = 110$ mm from the zero-moment position to the interior support.

Fig. 12 represents the slip and horizontal shear flow distribution. Notably, the slip distribution show a good agreement between both analytical results in spite of using the different solution procedure. Fig. 12(a) shows that, in the case of the continuous beam, the slip values developed at some points within the span (point A in Fig. 12(a)) are larger than those at the far end positions(point B in Fig. 12(a)). Fig. 12(b) shows that direct application of a linear elastic analysis for the horizontal shear flow $q(x) = V(x) \cdot Q_T/I_T$ assuming a full connection along the interface to a partially composite beam may cause improper arrangement of the shear connectors, where the subscript T denotes the transformed section. A beam with a partial shear connection or with flexural shear studs represents the four extremal values of horizontal shear flow at the far end supports and two points within the span, while a beam with full shear connections represents a constant distribution between the loading point and support. Since the partially composite beams give very little horizontal shear flow at the interior support, the difference in horizontal shear force will be greatest at this position, and this will accompany an excessive arrangement of shear connectors at the region around the interior support in the case of partially composite beams. Accordingly, the slip behavior should be considered in order to reach a more reasonable shear design of partially composite beams.

Table 1 Material properties of test specimens

Specimen			E1	CTB4	SCP 107
Concrete	Modulus of elasticity (MPa)		33000	33000	43000
	Compressive strength (MPa)		32.7	34.0	48.32
	Tensile strength (MPa)		3.07	3.15	2.96
Steel	Modulus of elasticity (MPa)		206000	206000	210000
	Yield stress (MPa)	Flange	250	236	460
		Web	297	238	
	Ultimate tensile stress (MPa)	Flange	465	393	600
		Web	460	401	

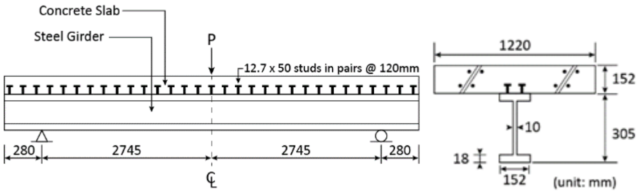

Fig. 13 Simply supported composite beam

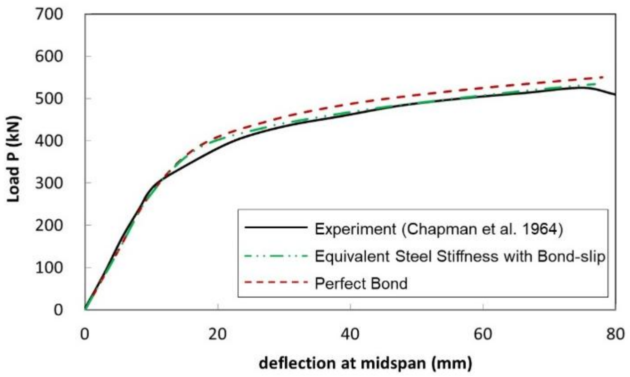

Fig. 14 Load-deflection relation of beam E1

5. Numerical applications

Additional comparison of the introduced numerical model with experimental data is conducted for three different steel-concrete composite structures that represent typical structural behaviors according to the bond-slip characteristics. These specimens are Beam E1, Beam CTB4, and Sandwich Plate experimented by Chapman and Balakrishnan (1964), Ansourian (1981), and Shin and Hwang (2016), respectively. The material properties of each specimen are listed in Table 1, and the finite element and its mesh size adopted in numerical modeling of each specimen are the same as those mentioned before (see 4. Experimental Verification).

The first example structure is a simply supported one-span beam subjected to a concentrated load P at the midspan. The details of the geometry including the placement of the shear studs and cross-sectional dimensions are shown in Fig. 13.

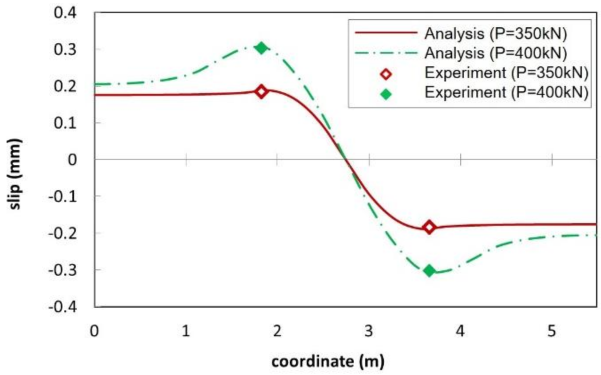

Fig. 15 Slip distribution of beam E1 along the span

Fig. 14 shows a comparison of the numerical results with experimental data (Chapman and Balakrishnan 1964) for the midspan deflection. Good agreement between the experiment and analysis is observed, regardless of the consideration of the bond-slip effect along the interface. In particular, the numerical results obtained by considering the bond-slip effect and by the perfect bond assumption are almost the same, and this result seems to be caused by the location of the interface, where bond-slip between the steel and concrete components is expected. Since the interface is located very closely to the centroid of a composite section in the case of this example structure, relatively large slip cannot develop under the flexural behavior.

The bond-slip behavior can also be evaluated on the basis of the introduced numerical model even though the developed slip is expected to be small. Fig. 15 represents the bond-slip distribution along the span with an increase of the applied load. As shown in this figure, the slip distribution is enlarged in proportion to the magnitude of the applied load up to reaching the yielding of the steel girder, but the yielding of the girder accompanies larger slip at the interface and the nonlinear slip distribution as well, because the flexural deformation rapidly increases after yielding of the steel beam.

The next example structure is a two-span continuous composite beam subjected to two identical concentrated loads at each midspan, and details of this specimen are presented in Fig. 16. The responses represented in Fig. 17 compare the load-displacement relations obtained by the proposed numerical model with the experimental data, and

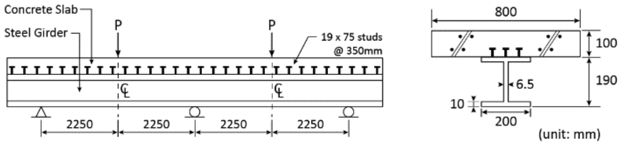

Fig. 16 Two span continuous composite beam CTB4

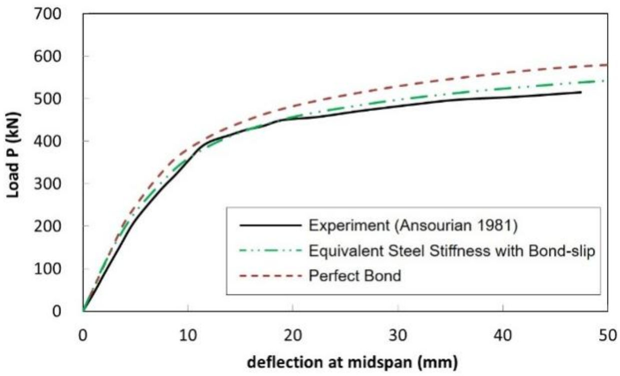

Fig. 17 Load-deflection relation of beam CTB4

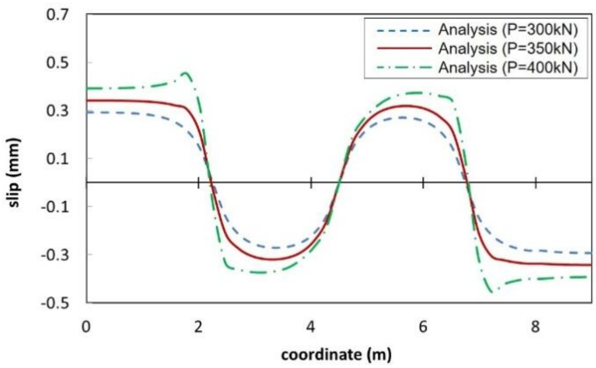

Fig. 18 Slip distribution of beam CTB4 along the span

the bond-slip distribution along the span with an increase of the applied load is represented in Fig. 18. The results of the proposed numerical model, which include the partial bond-slip effect display very satisfactory agreement with the experimental data. Meanwhile, the numerical results without consideration of the bond-slip effect upon the perfect bond assumption represent an overestimation of the resisting capacity of the example structure. In particular, the difference between the two numerical results of considering and ignoring the bond-slip effect increases when compared with that obtained for the previous example structure Beam E1. This appears to be caused by the dominant slip behavior developed at the regions located nearby the interior support.

The same comparison is conducted for a steel-concrete panel (SCP). This panel is designed to test the flexural resisting capacity of a SCP because it will be used as a part of a composite liquid natural gas (LNG) tank. To reserve the composite action between the exterior steel plates and the interior concrete matrix, steel studs are uniformly placed in 80 mm × 80 mm grids except the corner studs, as shown in

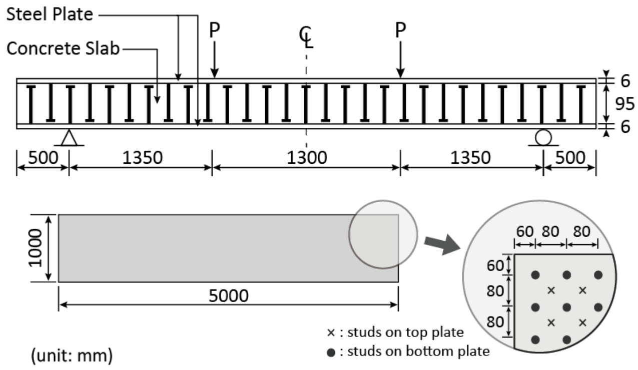

Fig. 19 Geometry and section dimensions for SCP

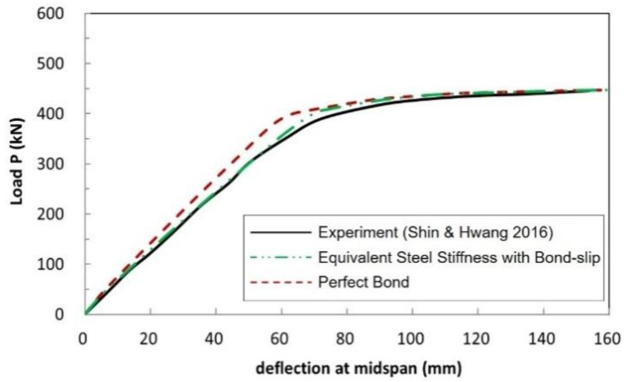

Fig. 20 Load-deflection relation of SCP

Fig. 19. Two concentrated loads are symmetrically applied, and details related to the composition of the SCP section can be found in Fig. 19. As shown in Fig. 19, steel plates are placed at the bottom and top surfaces, so the strength reduction due to buckling of the steel plate on top surface is investigated. Nevertheless, the yield strength of steel is not modified because the specimen has a dense arrangement of studs and critical stress is larger than the yield strength of the steel.

Fig. 20 compares the analytical and experimental results for the midspan deflection. Similarly to the previous results, the inclusion of the bond-slip effect gives more improved results in estimating the structural response with load increase up to the ultimate load. In particular, this figure shows that SCP is still dominantly affected by the bond-slip effect in spite of the placement of many shear studs. However, because of the lack of experimental data for the slip behavior, additional comparison related to the slip distribution along the span was not conducted. More examples of structural behavior of SCP can be found in the companion paper. (Lee *et al*. 2019)

6. Conclusions

This paper introduces a simplified numerical model to take into account the bond-slip effect without using a double node in steel-concrete composite structures. Unlike many other numerical models that have restrictions in the numerical modeling when the bond-slip effect is considered, the proposed model, which uses the equivalent modulus of elasticity for steel, can yield significant savings in the number of nodes needed to account for the slip behavior and can be easily implemented into commercialized programs including ABAQUS and ADINA as a user defined material model. The validity of the proposed numerical model is verified through correlation studies between the analytical results and experimental data, and the additional numerical analyses yield the following conclusions: (1) the inclusion of the bond-slip effect is important to precisely simulate the structural response of partially bonded composite flexural structures; (2) the bond-slip effect is minor when the the steel-concrete interface is located close to the centroid of a composite section; and (3) the proposed numerical model can be effectively used to simulate the bond-slip behavior, while remarkably reducing the complexity in numerical modeling of structures.

Acknowledgments

This work was supported by the National Research Foundation of Korea (NRF) Grant funded by the Korean Government (MSIT) (No. 2017R1A5A1014883).

References

ADINA (2015), ADINA Handbook system 9.1, ADINA R&D, Inc.

AISC 360 (2010), Specification for Structural Steel Buildings, American Institute of Steel Construction; Chicago, USA.

Ansourian, P. (1981), "Experiments on continuous composite beams", No. Res Rpt. R 384 Monograph.

Bärtschi, R. and Fontana, M. (2006), "Composite beams with nonlinear material and connector behaviour for low degrees of partial shear connection", *Compos. Constr. Steel Concrete V*, 573-582. https://doi.org/10.1061/40826(186)54

Bathe, K.J. (2007), *Finite Element Procedures*, Klaus-Jurgen Bathe.

Bonilla, J., Bezerra, L.M., Mirambell, E. and Massicotte, B. (2018), "Review of stud shear resistance prediction in steel-concrete composite beams", *Steel Compos. Struct., Int. J.*, **27**(3), 355-370. https://doi.org/10.12989/scs.2018.27.3.355

Chapman, J.C. and Balakrishnan, S. (1964), "Experiments on composite beams", *Struct. Engr.*, **42**(11), 369-383.

Chopra, A.K. (2007), Dynamics of Structures : Theory and Applications to Earthquake Engineering, Pearson Education

de Groot, A.K., Kusters, G.M.A. and Monnier, T. (1981), "Concrete mechanics. Part B: Numerical modelling of bond-slip behvaviour", NASA STI/Recon Technical Report N 82.

Dehestani, M. and Mousavi, S.S. (2015), "Modified steel bar model incorporating bond-slip effects for embedded element method", *Constr. Build. Mater.*, **81**, 284-290. https://doi.org/10.1016/j.conbuildmat.2015.02.027

Dezi, L., Ianni, C. and Tarantino, A.M. (1993), "Simplified creep analysis of composite beams with flexible connectors", *J. Struct. Eng.*, **119**(5), 1484-1497. https://doi.org/10.1016/j.conbuildmat.2015.02.027

Dias, M.M., Tamayo, J.L., Morsch, I.B. and Awruch, A.M. (2015), "Time dependent finite element analysis of steel-concrete composite beams considering partial interaction", *Comput. Concrete, Int. J.*, **15**(4), 687-707. https://doi.org/10.12989/cac.2015.15.4.687

Ding, F.X., Yin, G.A., Wang, H.B., Wang, L. and Guo, Q. (2017), "Behavior of headed shear stud connectors subjected to cyclic loading", *Steel Compos. Struct., Int. J.*, **25**(6), 705-716. https://doi.org/10.12989/scs.2017.25.6.705

El-lobody, E. and Lam, D. (2002), "Modelling of headed stud in steel-precast composite beams", *Steel Compos. Struct., Int. J.*, **2**(5), 355-378. https://doi.org/10.12989/scs.2002.2.5.355

Eurocode 4 (2004), Design of composite steel and concrete structures Part 1-1 : General rules and rules for buildings. European Committee for Standardization; Brussels, Belgium.

Gara, F., Ranzi, G. and Leoni, G. (2006), "Displacement-based formulations for composite beams with longitudinal slip and vertical uplift", *Int. J. Numer. Methods Eng.*, **65**(8), 1197-1220. https://doi.org/10.1002/nme.1484

Gattesco, N. (1999), "Analytical modeling of nonlinear behavior of composite beams with deformable connection", *J. Constr. Steel Res.*, **52**(2), 195-218. https://doi.org/10.1016/S0143-974X(99)00026-7

Hwang, J.W. and Kwak, H.G. (2013), "Improved FE model to simulate interfacial bond-slip behavior in composite beams under cyclic loadings", *Comput. Struct.*, **125**, 164-176. https://doi.org/10.1016/j.compstruc.2013.04.020

Kent, D.C. and Park, R. (1971), "Flexural members with confined concrete", *J. Struct. Div.*, **97**(7), 1969-1990.

Keuser, M and Mehlhorn, G. (1988), "Finite element models for bond problems", *J. Struct. Eng.*, **113**(10), 2160-2173. https://doi.org/10.1061/(ASCE)0733-9445(1987)113:10(2160)

Kwak, H.G. and Hwang, J.W. (2010), "FE model to simulate bond-slip behavior in composite concrete beam bridges", *Comput. Struct.*, **88**(17-18), 973-984. https://doi.org/10.1016/j.compstruc.2010.05.005

Kwak, H.G. and Kim, S.P. (2001), "Bond-slip behavior under monotonic uniaxial loads", *Eng. Struct.*, **23**(3), 298-309. https://doi.org/10.1016/S0141-0296(00)00008-0

Kwak, H.G. and Kim, S.P. (2010), "Simplified monotonic moment-curvature relation considering fixed-end rotation and axial force effect", *Eng. Struct.*, **32**(1), 69-79. https://doi.org/10.1016/j.engstruct.2009.08.017

Lam, D. and El-Lobody, E. (2005), "Behavior of headed stud shear connectors in composite beam", *J. Struct. Eng.*, **131**(1), 96-107. Lowes, L.N., Moehle, J.P. and Govindjee, S.

Lee, W.H., Kwak, H.G. and Kim, J.R. (2019), "Bond-slip effect in steel-concrete composite flexural members: (2) Improvement of shear stud spacing in SCP", *Steel Compos. Struct., Int. J.*, 32(4), 549-557. https://doi.org/10.12989/scs.2019.32.4.549

Lin, J.-P., Wang, G., Bao, G. and Xu, R. (2017), "Stiffness matrix for the analysis and design of partial-interaction composite beams", *Constr. Build. Mater.*, **156**, 761-772. https://doi.org/10.1016/j.conbuildmat.2017.08.154

Lizhong, J., Zhiwu, Y., Hua, C. and Zhongwu, L. (2008), "Effect of shear connection degree on seismic resistant performance of steel-concrete composite beams", *Build. Struct.*, **3**, 15.

Loh, H.Y., Uy, B. and Bradford, M.A. (2004), "The effects of partial shear connection in the hogging moment regions of composite beams Part I - Experimental study", *J. Constr. Steel Res.*, **60**(6), 897-919. https://doi.org/10.1016/j.jcsr.2003.10.007

Lowes, L.N., Moehle, J.P. and Govindjee, S. (2004), "Concrete-steel bond model for use in finite element modeling of reinforced concrete structures", *Struct. Journal*, **101**(4), 501-511.

Lubliner, J., Oliver, J., Oller, S. and Oñate, E. (1989), "A plastic-damage model for concrete", *Int. J. Solids Struct.*, **25**(3), 299-326. https://doi.org/10.1016/0020-7683(89)90050-4

Menzies, J.B. (1971), "CP117 and shear connectors in steel-concrete composite beams made with normal-density or lightweight concrete", *Struct. Engr.*, **49**(3), 137-154.

Oehlers, D.J. and Bradford, M.A. (1999), *Elementary behaviour of composite steel and concrete structural members*, Butterworth-Heinemann.

Oehlers, D.J. and Bradford, M.A. (2013), *Composite steel and concrete structural members* : *fundamental behaviour*, Elsevier

Oehlers, D.J. and Coughlan, C.G. (1986), "The shear stiffness of stud shear connections in composite beams", *J. Constr. Steel Res.*, **6**(4), 273-284. https://doi.org/10.1016/0143-974X(86)90008-8

Queiroz, F.D., Vellasco, P.C.G.S. and Nethercot, D.A. (2007), "Finite element modelling of composite beams with full and partial shear connection", *J. Constr. Steel Res.*, **63**(4), 505-521. https://doi.org/10.1016/j.jcsr.2006.06.003

Ranzi, G. and Zona, A. (2007), "A steel-concrete composite beam model with partial interaction including the shear deformability of the steel component", *Eng. Struct.*, **29**(11), 3026-3041. https://doi.org/10.1016/j.engstruct.2007.02.007

Roberts, T.M. (1985), "Finite difference analysis of composite beams with partial interaction", *Comput. Struct.*, **21**(3), 469-473. https://doi.org/10.1016/0045-7949(85)90124-5

Roberts, T.M., Helou, A.J., Narayanan, R. and Naji, F.J. (1995), "Design criteria for double skin composite immersed tunnels", *Proceeding of the Third International Conference on Steel and Aluminium Structures*, Istanbul, Turkey, pp. 507-514.

Scott, B.D., Park, R. and Priestley, M.J.N. (1982), "Stress-Strain Behavior of Concrete Confined by Overlapping Hoops at Low and High Strain Rates", *J. Am. Concrete Inst.*, **79**(1), 13-27.

Shim, C.S., Lee, P.G. and Yoon, T.Y. (2004), "Static behavior of large stud shear connectors", *Eng. Struct.*, **26**(12), 1853-1860. https://doi.org/10.1016/j.engstruct.2004.07.011

Shin, D.K. and Hwang, Y.Y. (2016), "An experimental study on bending capacity of SC(steep plate) panel", *Proceedings of Conference on Korean Concrete Institute* (*KCI*), **28**(1), 1-2.

Simulia, D. (2017), Abaqus 6.17 Documentation, DS SIMULIA Corp., USA

Sousa Jr, J.B.M. and da Silva, A.R. (2007), "Nonlinear analysis of partially connected composite beams using interface elements", *Finite Elem. Anal. Des.*, **43**(11-12), 954-964. https://doi.org/10.1016/j.finel.2007.06.010

Wang, A.J. and Chung, K.F. (2008), "Advanced finite element modelling of perforated composite beams with flexible shear connectors", *Eng. Struct.*, **30**(10), 2724-2738. https://doi.org/10.1016/j.engstruct.2008.03.001

Winkler, B., Blanchi, P. and Siemens, M. (2006), "Nonlinear analysis of connectors applied on concrete composite constructions", *Comput. Concrete*, *Int. J.*, **3**(2-3), 91-102. https://doi.org/10.12989/cac.2006.3.2_3.091

Zhang, K., Varma, A.H., Malushte, S.R. and Gallocher, S. (2014), "Effect of shear connectors on local buckling and composite action in steel concrete composite walls", *Nuclear Eng. Des.*, **269**, 231-239. https://doi.org/10.1016/j.nucengdes.2013.08.035

CC